JACS
JOURNAL OF THE AMERICAN CHEMICAL SOCIETY

ARTICLE

pubs.acs.org/JACS

Thermochemistry of the Initial Steps of Methylaluminoxane Formation. Aluminoxanes and Cycloaluminoxanes by Methane Elimination from Dimethylaluminum Hydroxide and Its Dimeric Aggregates

Rainer Glaser* and Xinsen Sun

Department of Chemistry, University of Missouri, Columbia, Missouri 65211, United States

Supporting Information

ABSTRACT: Results are presented of ab initio studies at levels MP2(full)/6-31G* and MP2(full)/6-311G** of the hydrolysis of trimethylaluminum (TMA, **1**) to dimethylaluminumhydroxide (DMAH, **2**) and of the intramolecular 1,2-elimination of CH_4 from **2** itself to form methylaluminumoxide **3**, from its dimeric aggregate **4** to form hydroxytrimethyldialuminoxane **5** and dimethylcyclodialuminoxane **6**, and from its TMA aggregate **7** to form **8** and/or **9**, the cyclic and open isomers of tetramethyldialuminoxane, respectively. Each methane elimination creates one new Lewis acid site, and dimethylether is used as a model oxygen-donor molecule to assess the most important effects of product stabilization by Lewis donor coordination. It is found that the irreversible formation of aggregate **4** (ΔG_{298} = −29.2 kcal/mol) is about three times more exergonic than the reversible formation of aggregate **7** (ΔG_{298} = −9.9 kcal/mol), that the reaction free enthalpies for the formations of **5** (ΔG_{298} = −9.0 kcal/mol) and **6** (ΔG_{298} = −18.8 kcal/mol) both are predicted to be quite clearly exergonic, and that there is a significant thermodynamic preference (ΔG_{298} = −7.2 kcal/mol) for the formation of **6** over ring-opening of **5** to hydroxytrimethyldialuminoxane **10**. The mechanism for oligomerization is discussed based on the bonding properties of dimeric aggregates and involves the homologation of HO-free aluminoxane with DMAH (i.e., **9** to **13**), and any initially formed hydroxydialuminoxane **10** is easily capped to trialuminoxane **13**. Our studies are consistent with and provide support for Sinn's proposal for the formation of oligoaluminoxanes, and in addition, the results point to the crucial role played by the kinetic stability of **5** and the possibility to form cyclodialuminoxane **6**. Dialuminoxanes **9** and **10** are reversed-polarity heterocumulenes, and intramolecular O→Al dative bonding competes successfully with Al complexation by Lewis donors. Intramolecular O→Al dative bonding is impeded in cyclodialuminoxane **6**, and the dicoordinate oxygen in **6** is a strong Lewis donor. Ethylene polymerization catalysts contain highly oxophilic transition metals, and our studies suggest that these transition metal catalysts should discriminate strongly in favor of cycloaluminoxane-O donors even if these are present only in small concentrations in the methylaluminoxane (MAO) cocatalyst.

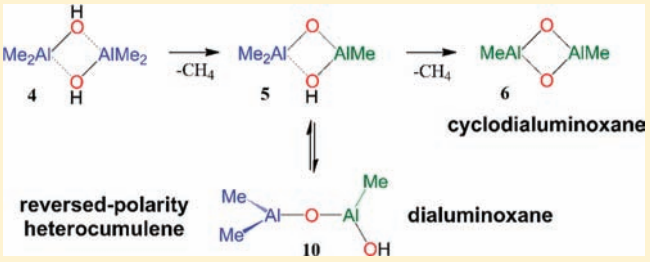

INTRODUCTION

The low-pressure polymerization of α-olefins with catalysts that combined aluminum alkyls and transition metal complexes (i.e., Ti, Zr) was discovered more than half a century ago, and the significance of the Ziegler−Natta polymerization[1] has steadily increased ever since.[2] The direct synthesis of triethylaluminum played a critical role for the initial success; trimethlyaluminum has since become available commercially;[3] and methylaluminoxane[4,5] (MAO) is most usually employed as cocatalyst.[6] A major advancement in transition metal catalysts occurred in the 1990s with reports by the groups of Brookhart[7,8] and Gibson[9] that described first examples of a new generation of homogeneous catalysts for ethylene polymerization. The precatalysts are neutral Fe(II) and Co(II) complexes formed by addition of tridentate pyridine bisimine ligands to the appropriate metal salt. The precatalysts are employed in nonpolar organic solvents (toluene, isobutane) in the presence of a very large excess (100−1000 equiv) of MAO as cocatalyst. The iron catalysts showed better activities in both studies, and their performance parameters were comparable to the most active Ziegler−Natta catalysts. More recently, Sun and co-workers explored structurally similar bidentate bis(imino)pyridyl Fe(II) complexes,[10] and tridentate 2,8-bis(imino)quinoline Fe(II) complexes,[11] and related systems with nickel[12,13] and titanium[14,15] also have been studied.

While the organometallic precatalysts are well characterized, very little is known about the structure(s) and the function(s) of the active MAO species. Methylaluminoxane (MAO) is a generic term used to describe the products of "controlled" hydrolysis of trimethyaluminum (TMA, Me_3Al), and modified methylaluminoxane

Received: October 20, 2010
Published: August 05, 2011

Scheme 1. MAO Compounds Discussed by Barron, Pasynkiewicz, Sinn, Ziegler, Hall, and Linnolathi

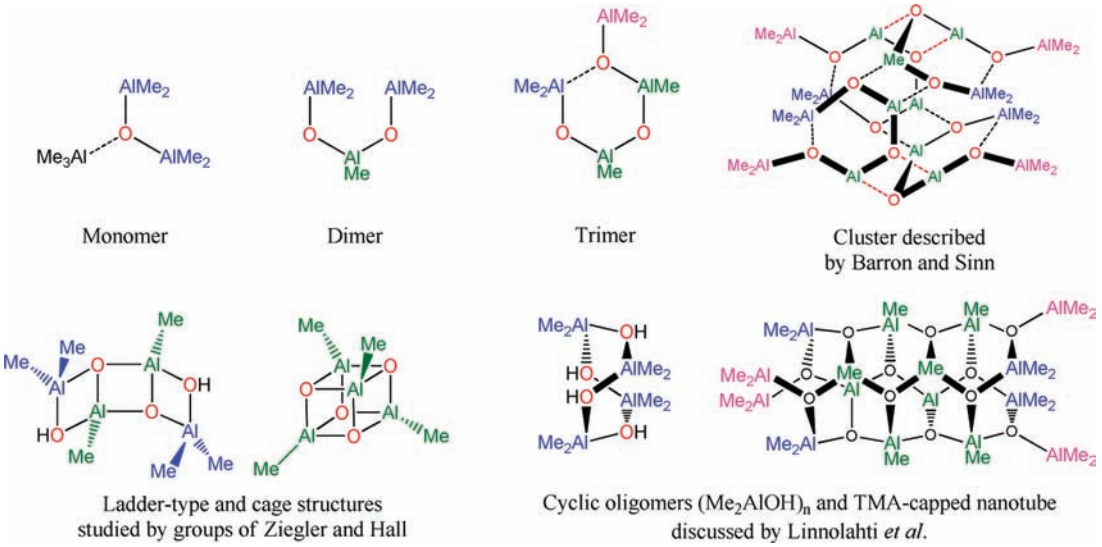

(MMAO) is obtained by hydrolysis of TMA with admixtures of other trialkylaluminum compounds (e.g., tBu_3Al). The compositions of MAO and MMAO are unknown, and they depend on their formation processes. In the BASF process, for example, MAO is prepared by addition of TMA to a slurry of $CuSO_4 \cdot 5H_2O$ in toluene.[16] In patents by Ethyl Corporation, the synthesis of MAO is described by reaction of TMA with the hydrate of an alkali or alkaline earth metal hydroxide or halide, and the TMA/MX-hydrate ratio may vary between 2 and 1/2.[17] In his recent review,[4] Severn wrote that "apart from residual TMA, no other structural components or specific molecules have been unambiguously isolated and identified". Still, one can begin with reasonable assumptions as to the types of reactions which occur during hydrolysis of TMA. There is no doubt that hydrolysis of alkyl−Al bonds will result in the formation of HO−Al bonds, the release of alkanes, and the formation of acyclic and cyclic systems with Al−O−Al bridges by further inter- and intramolecular alkane elimination, and the experimental studies of aluminoxanes by Barron,[18−20] Pasynkiewicz,[21] and Sinn[22] suggest a plethora of chain, ladder, and cage structures (Scheme 1). Theoretical studies by Ziegler et al.,[23] by Hall and co-workers,[24] and by Linnolahti et al.[25] explored possible species with ladder and cage structures derived from dimethylaluminum hydroxide (DMAH).

In his seminal 1995 paper,[21] Sinn explored the structure of MAO formed from TMA on the surface of water ice at −40 °C, and the experimental results are consistent with a $[Al_4O_3(Me)_6]_4$ cage cluster originally proposed by Barron.[18] The experiments showed that the cluster may contain a molecule of TMA or solvent (ether, 1,4-dioxane, THF), and the dominant species in toluene and ether solution are $[Al_4O_3(Me)_6]_4 \cdot (TMA)_x$ (x = 0−4) and $[Al_4O_3(Me)_6]_4 \cdot (OEt_2)_2$, respectively. Sinn convincingly argued for a cage structure formed by aggregation of four $Al_4O_3Me_6$ trimers (Scheme 1). The proposals by Hall[22] and by Linnolahti[23] for potential MAO species bypass the $Al_4O_3Me_6$ trimer. Hall discussed DMAH aggregates $(Me_2AlOH)_n$ (n = 2, 3, ...) and showed how the higher aggregates can lead to ladder-like structures by trans-annular CH_4 elimination and that cage-like structures $(MeAlO)_n$ may result by reaction between the termini of ladder-type species. Linnolahti considered the coupling of cyclic oligomers $(Me_2AlOH)_n$ to nanotubular structures with concomitant CH_4 elimination with dodecamer $Al_{16}O_{12}Me_{24}$ as the thermodynamic sink. Hall and Linnolahti invoke intermolecular CH_4 elimination to grow the aggregates, and Hall also invokes intramolecular 1,n-elimination (n = 4, 5, ...) to close cage structures.

We present here the results of ab initio studies of intramolecular 1,2-elimination of CH_4 from dimethylaluminumhydroxide (DMAH, **2**) itself to form methylaluminumoxide **3**, from its dimeric aggregate **4** to form **5** and/or **6**, and from its TMA aggregate **7** to form **8** and/or **9** (Scheme 2). Sinn discussed $O(AlMe_2)_2$ as "the monomer" following polyether nomenclature.[26] We also employ the nomenclature for heterogeneous hydrides[27] and refer to $Me_2Al-O-AlMe_2$ as permethyldialuminoxane, and **8** and **9** are its cyclic and open isomers, respectively. In analogy, the hydroxytrimethyldialuminoxane **10** is the acyclic isomer of **5**. Aluminoxanes contain strong Lewis acidic and Lewis basic sites, and it is likely that their formations, their structures, and their functions are affected by aggregation and solvation. We are considering the smallest possible cyclic aggregates of DMAH, **4** and **7**, because entropy favors these aggregates over larger cyclic aggregates. Each CH_4 elimination creates one new Lewis acid site, and the elimination product thus may be stabilized by aggregation with an available Lewis donor.[28] Aluminum is highly oxophilic,[29] and product stabilization can be provided by other aluminoxanes and/or by donor molecules (i.e., water, ether),[30] and/or anions (i.e., halides, sulfates, etc.) present during MAO formation. In the present study, dimethylether serves as a simple donor molecule to assess the most important product stabilization effects by Lewis donor coordination (Scheme 3). While the results of our studies are most directly applicable to ether solutions of aluminoxanes, we will emphasize throughout this article that we employ dimethylether as a simple donor molecule and that the discussion is therefore relevant for reaction systems that do not contain ethers but other O-donor molecules. At the beginning, we considered the study of the hydrates in the hope that we could learn about the intermediates of MAO formation and about donor-stabilized MAO species at the same time. We abandoned that approach because the hydrate complexes feature $H_2O \cdots Al$ dative bonding and also hydrogen-bonding between water and O-sites in the MAO species. The focus of the present paper is on the comparison of the thermodynamic stabilities of

Scheme 2. Formation of Dimethylcyclodialuminoxane 6 by Two-Fold 1,2-Elimination of CH_4 from the Cyclic Dimer 4 of Dimethylaluminum Hydroxide 2[a]

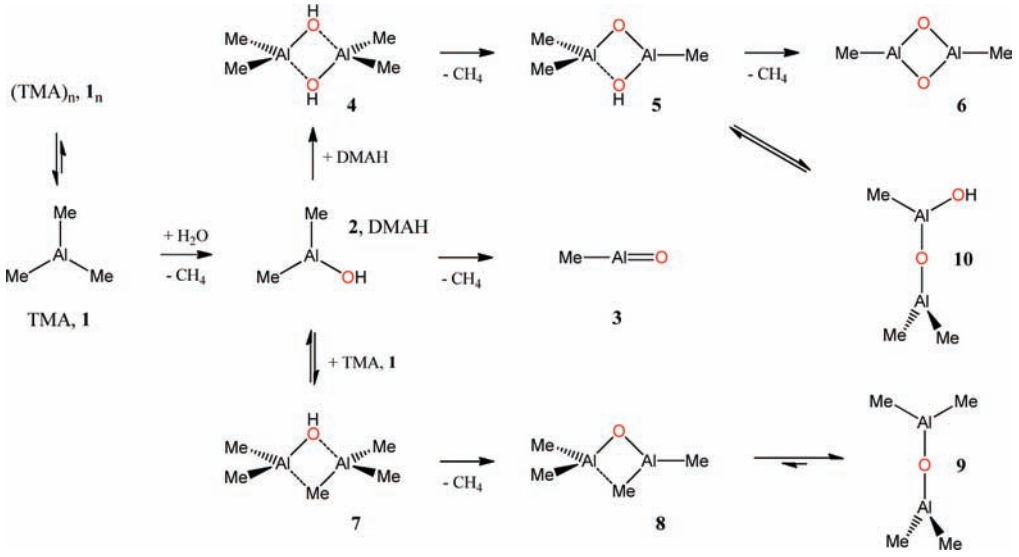

[a] Methyl-bridged cycloadduct **7** results by aggregation of TMA with **2**, and 1,2-elimination of CH_4 from **7** leads to tetramethyldialuminoxane **9**, the Sinn monomer. Cycloadduct **5** is in equilibrium with hydroxytrimethyldialuminoxane **10**.

Scheme 3. Models for Lewis Donor Stabilized Aluminoxanes: O-Donor Coordinated Structures of 5−7 and 9 and 10

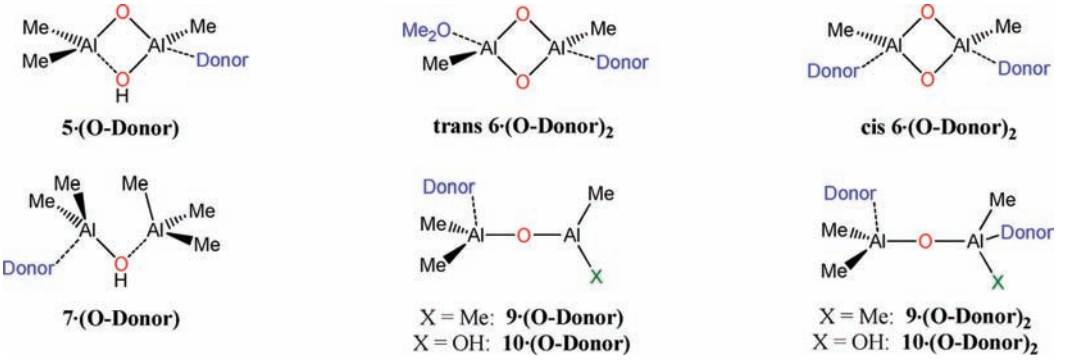

different MAO species (rather than about the details of the reactions that connect the various MAO species), and for this purpose OMe_2 is a suitable donor to model donor-stabilized MAO species.

COMPUTATIONAL METHODS

Computations were performed with Gaussian03[31] on the 64-processor SGI Altix system of the UM Research Computing facilities. Potential energy surface (PES) analyses[32] were performed with second-order Møller−Plesset perturbation theory (MP2)[33] with all electrons included in the active space and in conjunction with the 6-31G* and 6-311G** basis sets.[34] Vibrational analyses were carried out analytically for each stationary structure at the level of optimization to compute vibrational frequencies and molecular thermal energies, enthalpies, and entropies. Molecular models of stationary structures are shown in the figures, and Cartesian coordinates of all optimized structures are provided as Supporting Information. Total energies E_{tot}, vibrational zero-point energies (VZPE), thermal energies (TE), molecular entropies (S), and dipole moments (μ) are documented in the Supporting Information as well. Isomer preference energies, activation, and reaction energies are discussed, and in Table 1 we report relative energies ΔE, enthalpies, $\Delta H_0 = \Delta(E + \text{VZPE})$ and $\Delta H_{298} = \Delta(E + \text{TE})$, and free enthalpies $\Delta G = \Delta(E + \text{TE} - 298.15 \cdot S)$.

All structures were computed at the MP2(full)/6-31G* level, and we discuss the results obtained at this level. The quality of this theoretical level is well established, and its economy allows for the computations of larger MAO systems. Nevertheless, we realize that the use of larger basis sets improves the Hartree−Fock wave functions especially of polar and strained molecules and that the increased virtual space provides for a better accounting of changes in electron correlation that accompany reactions. To assess basis set effects on the intrinsic reactions energies, **1**−**10** were computed again at the MP2-(full)/6-311G** level. Using all pairs of reaction energies computed at the levels MP2(full)/6-31G* (Method 1) and MP2(full)/6-311G** (Method 2),[35] linear correlation results in the equations $\Delta H_{298}(\text{M2}) = 1.025 \cdot \Delta H_{298}(\text{M1}) + 5.890$ ($R^2 = 0.993$) and $\Delta G_{298}(\text{M2}) = 1.014 \cdot \Delta H_{298}(\text{M1}) + 5.534$ ($R^2 = 0.981$). For reactions that involve ether donor coordination, the values reported in Table 1 were determined by combining the respective value computed for the donor-free reaction at the MP2(full)/6-311G** level with the donor-coordination effect computed at the MP2(full)/6-31G* level.

Table 1. Computed Relative and Reaction Energies (kcal/mol)

		method 1				method 2			
eq	reaction/process	ΔE	ΔH_0	ΔH_{298}	ΔG_{298}	ΔE	ΔH_0	ΔH_{298}	ΔG_{298}
	TMA Hydrolysis								
1	**1** + H_2O → **2** + CH_4	−42.86	−41.37	−41.88	−41.84	−36.71	−35.32	−35.95	−33.15
2	**2** → **3** + CH_4	40.96	40.31	40.13	34.72	47.38	46.50	46.34	38.68
3	**1** + H_2O → **3** + 2 CH_4	−1.90	−1.06	−1.75	−7.12	10.67	11.19	10.39	5.52
4	**1** + OMe_2 → **1**·OMe_2	−23.71	−21.74	−21.47	−7.93				
5	**2** + OMe_2 → **2**·OMe_2	−24.98	−23.22	−22.82	−8.02				
6	**3** + OMe_2 → **3**·OMe_2	−27.15	−25.36	−24.85	−14.28				
7	**3** + 2 OMe_2 → **3**·$(OMe_2)_2$	−49.97	−46.52	−45.56	−22.82				
8	**3**·OMe_2 + OMe_2 → **3**·$(OMe_2)_2$	−22.82	−21.16	−20.71	−8.54				
9	**1**·OMe_2 + H_2O → **2**·OMe_2 + CH_4	−44.12	−42.86	−43.24	−41.93	−37.97	−36.81	−37.31	−33.24
10	**2**·OMe_2 + OMe_2 → **3**·$(OMe_2)_2$ + CH_4	15.96	17.00	17.40	19.92	22.38	23.19	23.61	23.88
11	**1**·OMe_2 + H_2O + OMe_2 → **3**·$(OMe_2)_2$ + 2 CH_4	−28.16	−25.85	−25.84	−22.01	−15.59	−13.60	−13.70	−9.37
	TMA Aggregation								
12	2 **1** → $(\mathbf{1})_2$, cyclic	−21.40	−18.73	−19.12	−1.24	−20.65	−18.02	−18.46	−0.01
13	2 **1** → $(\mathbf{1})_2$, acyclic	−5.27	−4.27	−3.32	6.56	−5.87	−4.74	−3.88	6.43
14	2 **1** + OMe_2 → $(\mathbf{1})_2$·OMe_2, cyclic	−27.55	−24.05	−23.32	3.22	−26.80	−23.34	−22.66	4.45
15	2 **1** + OMe_2 → $(\mathbf{1})_2$·OMe_2, acyclic	−32.28	−29.02	−28.04	−2.25	−32.88	−29.49	−28.60	−2.38
16	2 **1** + OMe_2 → $(\mathbf{1})_2$·OMe_2, sandwich	−34.24	−29.96	−29.80	0.58				
	Methane 1,2-Elimination in Cycloadducts								
17	**4** → **5** + CH_4	14.14	12.85	13.07	2.51	19.83	18.73	18.68	9.06
18	**5** → **6** + CH_4	−0.04	−0.24	−0.55	−11.03	8.32	8.71	7.86	−0.07
19	**4** → **6** + 2 CH_4	14.10	12.61	12.52	−8.52	28.15	27.43	26.54	8.99
20	**7** → **9** + CH_4	−7.98	−9.45	−8.59	−23.61	−1.74	−3.53	−2.67	−19.24
21	**5** + OMe_2 → **5**·(OMe_2)	−33.00	−30.95	−30.64	−18.09				
22	*trans*-**6**·$(OMe_2)_2$ → *cis*-**6**·$(OMe_2)_2$	3.53	3.44	3.45	3.72				
23	**6** + 2 OMe_2 → **6**·$(OMe_2)_2$	−58.44	−54.87	−53.96	−27.79				
24	**7** + OMe_2 → **7**·(OMe_2)	−17.63	−16.42	−15.40	−15.58				
25	**9** + OMe_2 → **9**·(OMe_2)	−24.71	−23.01	−22.62	−9.69				
26	**9** + 2 OMe_2 → **9**·$(OMe_2)_2$	−48.07	−44.82	−43.94	−18.92				
27	**4** + OMe_2 → **5**·(OMe_2) + CH_4	−18.86	−18.10	−17.57	−15.58	−13.17	−12.22	−11.96	−9.03
28	**5**·(OMe_2) + OMe_2 → **6**·$(OMe_2)_2$ + CH_4	−25.48	−24.16	−23.87	−20.72	−17.12	−15.21	−15.46	−9.76
29	**4** + 2 OMe_2 → **6**·$(OMe_2)_2$ + 2 CH_4	−44.34	−42.26	−41.44	−36.30	−30.29	−27.44	−27.42	−18.79
30	**7** + OMe_2 → **9**·(OMe_2) + CH_4	−32.68	−32.45	−31.22	−33.30				
31	**7** + 2 OMe_2 → **9**·$(OMe_2)_2$ + CH_4	−56.20	−54.41	−52.68	−42.59				
32	**7**·(OMe_2) → **9**·(OMe_2) + CH_4	−15.05	−16.03	−15.82	−28.17				
33	**7**·(OMe_2) + OMe_2 → **9**·$(OMe_2)_2$ + CH_4	−38.57	−37.99	−37.28	−37.46	−32.33	−32.07	−31.36	−33.09
	Cycloadduct Formation								
34	2 **2** → **4**	−65.48	−62.98	−63.14	−43.80	−61.63	−59.44	−59.29	−45.21
35	**2** + **3** → **5**	−92.30	−90.44	−90.21	−76.01	−89.18	−87.22	−86.96	−74.83
36	2 **3** → **6**	−133.30	−130.99	−130.90	−121.76	−128.24	−125.98	−125.83	−116.36
37	**1** + **2** → **7**	−41.17	−38.73	−39.04	−20.28	−39.37	−37.02	−37.22	−20.69
38	2 **2**·(OMe_2) → **4** + 2 OMe_2	−15.53	−16.54	−17.50	−27.76	−11.68	−13.00	−13.65	−29.17
39	**2**·(OMe_2) + **3**·$(OMe_2)_2$ → **5**·(OMe_2) + 2 OMe_2	−50.35	−51.65	−52.47	−63.26	−47.23	−48.43	−49.22	−62.08
40	2 **3**·$(OMe_2)_2$ → **6**·$(OMe_2)_2$ + 2 OMe_2	−91.79	−92.81	−93.74	−103.90	−86.73	−87.80	−88.67	−98.50
41	**1**·(OMe_2) + **2**·(OMe_2) → **7** + 2 OMe_2	7.52	6.22	5.25	−4.32	9.32	7.93	7.07	−4.73
42	**1**·(OMe_2) + **2**·(OMe_2) → **7**·(OMe_2) + OMe_2	−10.11	−10.20	−10.15	−9.46	−8.31	−8.49	−8.33	−9.87
	Ring-Opening of Cycloadduct **5**								
43	**5** → **10**	3.25	2.98	3.40	0.38	1.58	1.04	1.59	−2.22
44	**10** + OMe_2 → **10**·(OMe_2)	−26.92	−25.38	−24.81	−12.71				
45	**10**·(OMe_2) + OMe_2 → **10**·$(OMe_2)_2$	−50.44	−47.28	−46.29	−21.18				

dx.doi.org/10.1021/ja109457j |*J. Am. Chem. Soc.* 2011, 133, 13323–13336

Table 1. Continued

		method 1				method 2			
eq	reaction/process	ΔE	ΔH_0	ΔH_{298}	ΔG_{298}	ΔE	ΔH_0	ΔH_{298}	ΔG_{298}
46	**5**·(OMe_2) → **10**·(OMe_2)	9.33	8.55	9.23	5.77	7.66	6.61	7.42	3.17
47	**5**·(OMe_2) + OMe_2 → **10**·$(OMe_2)_2$	−23.52	−21.90	−21.48	−8.47	−25.19	−23.84	−23.29	−11.07
48	**10** → **6** + CH_4	−3.29	−3.22	−3.96	−11.41	6.73	6.70	5.88	−0.62
49	**10**·$(OMe_2)_2$ → **6**·$(OMe_2)_2$ + CH_4	−11.28	−10.82	−11.62	−18.02	−1.26	−0.90	−1.78	−7.23
	Isodesmic Reaction								
	2 + Me−Al═O → **1** + HO−Al═O					12.73	11.57	12.09	10.33
	Trialuminoxane Formation Reactions								
50	**9** + **2** → **11**	−53.30	−51.27	−51.41	−32.69				
51	**9** + **4** → **11** + **2**	12.18	11.70	11.75	11.13				
52	**9** + **7** → **11** + **1**	−12.13	−12.54	−12.36	−12.41				
53	**11** → **12** + CH_4	−4.57	−4.64	−5.45	−11.63				
54	**12** → **13**	9.83	8.69	10.22	0.60				
55	**9** + **2** → **13** + CH_4	−48.05	−47.22	−46.64	−43.72				
56	**2** + **2** → **10** + CH_4 (eqs 17 + 34 + 43)	−48.09	−47.15	−46.67	−40.91				
57	**9** + **2** → **14**	−13.78	−11.78	−11.84	4.88				
58	**9** + **4** → **14** + **2**	51.70	51.19	51.31	48.69				
59	**9** + **7** → **14** + **1**	27.39	26.95	27.20	25.15				
60	**10** + **1** → **14**	−14.84	−12.81	−12.81	1.89				
61	**10** + $(1)_2$ → **14** + **1**	−9.57	−8.54	−9.48	−4.66				
62	**14** → **13** + CH_4	−34.46	−35.44	−47.79	−48.60				
63	**10** + **1** → **13** + CH_4	−49.10	−48.26	−47.60	−46.70				
64	**2** + **1** → **9** + CH4 (eqs 20 + 37)	−49.15	−48.18	−47.63	−43.89				

RESULTS AND DISCUSSION

Methane Elimination from DMAH. The reaction of water with trimethylaluminum (TMA, **1**) affords dimethylaluminum-hydroxide (DMAH, **2**), and subsequent intramolecular CH_4 elimination from DMAH formally presents a path to the formation of methylaluminumoxide **3**. The computed structures of **1**−**3** and of their etherates are shown in Figure 1. The data computed for **1**·(OMe_2) agree very well with the measured ether binding energy (H_f = 21.92 ± 0.18 kcal/mol[36]) and with the gas phase structure[37] of **1**·(OMe_2). McMahon et al. reported the crystal structure of a related $R_3Al(R'OH)$ complex, $(tBu)_3Al[O(H)CH_2CH_2CH_2NMe_2]$.[38]

The reaction energies computed for reactions **1** + H_2O → **2** + CH_4 (eq 1) and **1**·OMe_2 + H_2O → **2**·OMe_2 + CH_4 (eq 9) are similar because of the comparable ether coordination energies of **1** and **2** (eqs 4 and 5), and the reactions are both highly exothermic and exergonic with reaction enthalpies and free reaction enthalpies of $\Delta H_{298} < -40$ and $\Delta G_{298} < -40$ kcal/mol.

The elimination reaction **2** → **3** + CH_4 (eq 2) naturally is endothermic and endergonic, and the pertinent question is whether the energy released in the reaction **1** + H_2O → **2** + CH_4 (eq 1) might suffice to make **3** accessible via the overall reaction **1** + H_2O → **3** + 2 CH_4 (eq 3). The assessment of the effects of donor stabilization is more difficult in this case because methylaluminum oxide **3** allows for primary Lewis donor coordination by two ether molecules (eqs 6−8). The first ether donor coordination of **3** is exergonic by $\Delta G_{298} = -14.3$ kcal/mol, and it is more than 6 kcal/mol higher in magnitude than the ether donor coordination free enthalpies of $\Delta G_{298} \approx -8$ kcal/mol of **1** and **2**. Note that most of this increase in free enthalpy is due to entropy effects. The second donor coordination of **3** is $\Delta G_{298} \approx -8.5$ kcal/mol and not much different from the ether donor coordination of **1** and **2**. The combined consequence (ca. 14.5 kcal/mol) of the stronger first donor coordination and of the additional second donor coordination reduces the endothermicity and the endergonicity of the reaction **2**·OMe_2 + OMe_2 → **3**·$(OMe_2)_2$ + CH_4 (eq 10) to ΔH_{298} = 16.0 kcal/mol and $\Delta G_{298} \approx$ 19.9 kcal/mol, respectively.

Our computations therefore suggest, and this result might not be intuitive, that the formation of **3** from **1** via the reaction **1**·OMe_2 + H_2O + OMe_2 → **3**·$(OMe_2)_2$ + 2 CH_4 (eq 11) is significantly exothermic and exergonic by $\Delta H_{298} = -28.2$ kcal/mol and $\Delta G_{298} \approx -22.0$ kcal/mol, respectively. While the formation of **2** is thermodynamically clearly favored over the formation of **3**, the important point here is the recognition that the formation of the latter cannot be ignored based on the (false) assumption that **3** might not be accessible thermodynamically.

Self-Aggregation of TMA. We used **1** and **1**·OMe_2 as references in the computation of the reaction energies of hydrolysis in the absence or presence of donor molecules (eqs 1 and 9), and these are the proper references because self-aggregation of TMA is insignificant. Almenningen et al. recognized that the equilibrium 2 TMA ⇄ $(TMA)_2$ is highly T-dependent in the gas phase ("trimethylaluminium gas at 60 °C and 30 mmHg consists of more than 97% dimers, while gas at 215 °C and the same pressure consists of more than 96% monomer") and were able to determine the structures of TMA and of its dimer in the gas phase.[39] The structures of TMA dimer and of trimeric aggregates $(TMA)_2$·OMe_2 were considered to make this point (Figure 2).

It is true that the structure of the cyclic TMA dimer is greatly stabilized by dative bonding ($\Delta H_{298} \approx -20$ kcal/mol, in excellent agreement with previous studies[40]); however, the

dx.doi.org/10.1021/ja109457j |J. Am. Chem. Soc. 2011, 133, 13323–13336

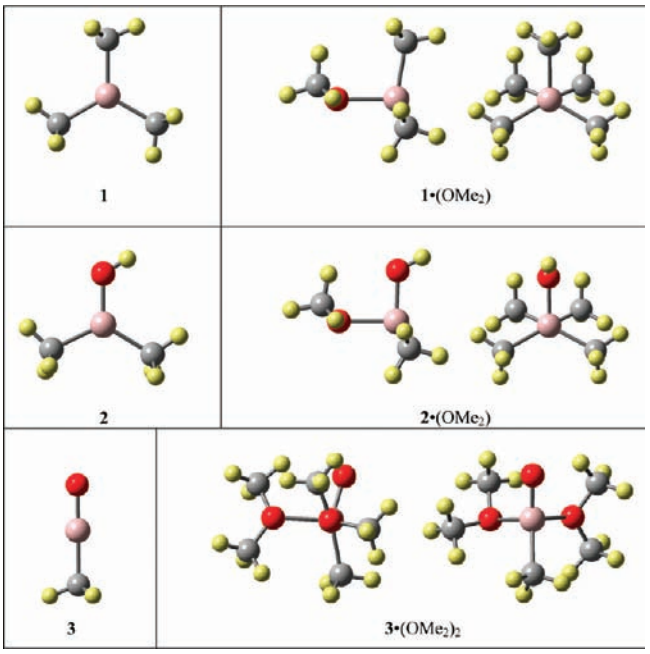

Figure 1. Computed structures of trimethylaluminum **1**, of dimethylaluminumhydroxide **2**, of methylaluminum oxide **3**, and of their etherates $\mathbf{1}\cdot OMe_2$, $\mathbf{2}\cdot OMe_2$, and $\mathbf{3}\cdot(OMe_2)_2$.

aggregation comes with an almost equally large entropy loss, and the formation of the cyclic TMA dimer is essentially thermoneutral (eq 12). The acyclic TMA dimer is a local minimum and about 8 kcal/mol less stable (eq 13). The cyclic dimer may form an aggregate with dimethylether as a very shallow minimum (eq 14), but this aggregate quickly collapses to the donor-coordinated acyclic TMA structure (eq 15). The formation of the sandwich structure seemed appealing because it allows for dative bonding between the donor-O and both Lewis acid sites, but again entropy renders this mode of aggregation essentially thermoneutral (eq 16). The entropy effects can be tempered if the chemistry is performed at lower temperature, but even at low reaction temperatures (i.e., 220 K) the TMA aggregation free enthalpy will not suffice to allow for aggregates with any significant lifetime.

Methane Elimination in the DMAH Dimer: Path to Cyclodialuminoxane 6? Instead of intramolecular CH_4 elimination to form **3**, DMAH might self-aggregate in **4**, and 2-fold CH_4 elimination may then lead to **5** and **6**. Molecule **5** is the cycloadduct of DMAH and **3**, and permethylcyclodialuminoxane **6** is the cyclodimer of **3**. The computed structures of **4**−**6** and of their etherates are shown in Figure 3.

The cyclic dimer $(t\mathrm{Bu_2AlOH})_2$ was characterized spectroscopically,[19b] and the crystal structure was reported of the cyclic trimer $(t\mathrm{Bu_2AlOH})_3$.[19a] Rogers et al. synthesized a large number of alkoxides $[Me_2Al(OR)]_n$ and found that the compounds either are purely dimeric in solution or that both dimers and trimers occur.[41] The most likely path for the formation of the trimer involves the addition of a monomer to a dimer, and the aggregation energy for the formation of **4** suggests that the conversion of the dimer to the trimer requires significant activation energy. Hence, the dimer should at least present a kinetic intermediate.

Structure **4** is C_2-symmetric, and the OH groups are placed in symmetrically bridging positions with $d(O-Al)$ = 1.895 Å and about 10% longer than the bond length $d(O-Al)$ = 1.729 Å in **2**. The hydroxyl H-atoms are out of the Al_2O_2 plane with angle $\angle(O\cdots O-H)$ = 139.8°. The ring angle at oxygen $\angle(Al-O-(H)-Al)$ = 98.4° is larger than the one at Al. Structure **6** is de facto C_s-symmetric, and all O−Al bond lengths are essentially the same, $d(O-Al)$ = 1.768 Å and about 8% longer than the respective bond length of 1.630 Å in **3**. The ring angle at oxygen $\angle(Al-O-Al)$ = 86.6° is smaller than the one at Al. Structure **5** is trapez-shaped; its base lengths are 1.697 and 2.051 Å; and its sides are 1.795 and 1.815 Å long. The "MeAlO" moiety in **5** is more **3**-like than in **6**, whereas the "Me_2AlOH" moiety in **5** is less **1**-like than in **4**. The ring angles in **5** are $\angle(Al-O(H)-Al)$ = 87.5° and $\angle(Al-O-Al)$ = 98.7°; the directions of the deviations from 90° angles are opposite to **4** and **6**, and the hydroxyl group lies in the Al_2O_2 plane. All of these structural observations inform and are consistent with the discussion of bonding (vide infra).

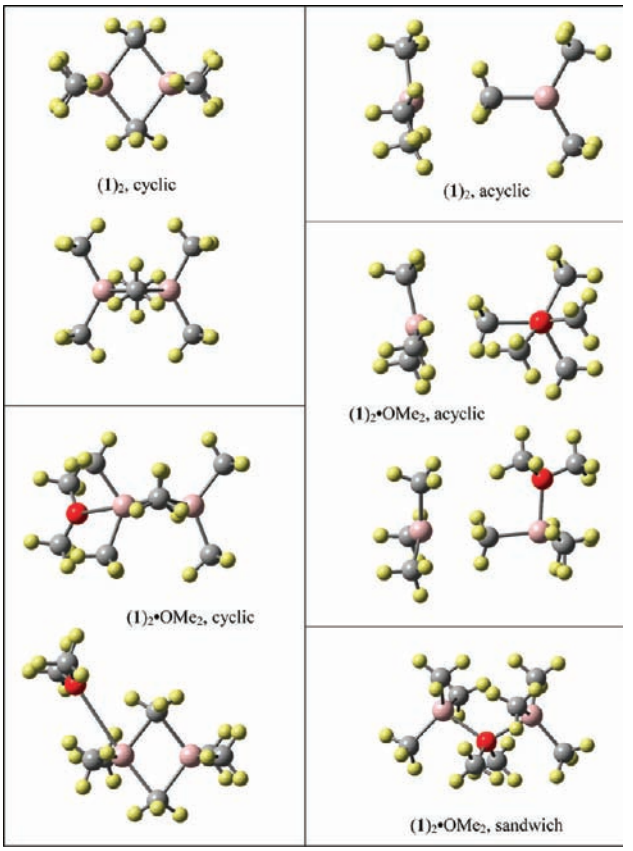

Figure 2. Computed structures of dimeric aggregates $(\mathbf{1})_2$ of TMA and of trimeric aggregates $(\mathbf{1})_2\cdot OMe_2$ that include two TMA molecules and one molecule of dimethylether.

We optimized the structures of etherates $\mathbf{5}\cdot(OMe_2)$ and $\mathbf{6}\cdot(OMe_2)_2$ and considered both the cis and trans structures of the latter (Figure 3). As with ether adducts of **1**−**3**, it is a common feature of these ether adducts that the ether−Al coordination is "wagged"; i.e., the solvated Al atom does not lie in the best plane of the ether molecule. This feature appears on the MP2(full)/6-31G* potential energy surface, while it is absent in RHF-level computations. Whenever possible, the wagging of the ether plane occurs in such a way as to approach one or both of the ether-methyls more closely to an Al-bound oxygen; see $\mathbf{2}\cdot(OMe_2)$ in Figure 1 and $\mathbf{5}\cdot(OMe_2)$ and trans $\mathbf{6}\cdot(OMe_2)_2$

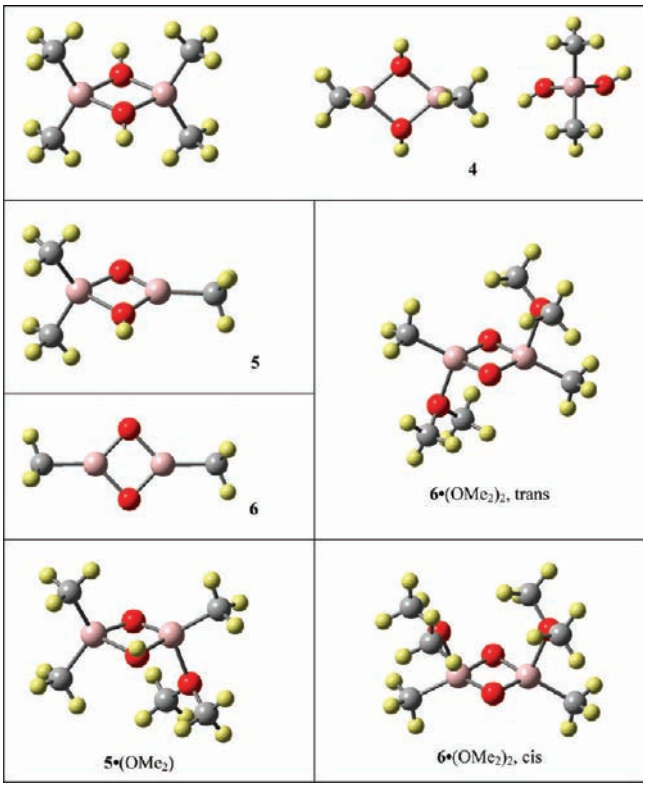

Figure 3. Computed structures of the dimer **4** of DMAH, of the cyclic aggregate **5** formed between DMAH and methylaluminumoxide and its etherate **5**·(OMe_2), and of dimethylcyclodialuminoxane **6** and its isomeric dietherate **6**·$(OMe_2)_2$.

in Figure 3. This intramolecular dispersion effect also is reflected in reduced $\angle$(O−Al···O_{ether}) angles; see **2**·(OMe_2) in Figure 1 in particular. The donor coordination enthalpies of of **5** and **6** (eqs 21 and 23) per ether donor are more than twice as large as for **2** and also exceed the complexation energy of **3**.

The first methane elimination reaction **4** → **5** + CH_4 (eq 17) is endothermic by ΔH_{298} = 13.2 kcal/mol, and it is only very slightly endergonic by ΔG_{298} = 2.5 kcal/mol. The second methane elimination reaction **5** → **6** + CH_4 (eq 18) is almost thermoneutral with ΔH_{298} = −0.6 kcal/mol, and it is quite clearly exergonic by ΔG_{298} = −11.0 kcal/mol. Hence, the overall reaction **4** → **6** + 2 CH_4 (eq 19) remains somewhat endothermic by ΔH_{298} = 12.5 kcal/mol, but it is clearly exergonic by ΔG_{298} = −8.5 kcal/mol. Primary donor coordination always favors elimination, and reactions 27−29 all are clearly exothermic and exergonic. For the reaction **4** + 2 OMe_2 → **6**·$(OMe_2)_2$ + 2 CH_4 (eq 29), we computed ΔH_{298} = −41.4 kcal/mol and ΔG_{298} = −36.3 kcal/mol.

Methane Elimination in TMA-Complexed DMAH: Dialuminoxane 9. DMAH can aggregate with TMA, which is available in large excess, and intramolecular CH_4 elimination might lead to tetramethyldialuminoxane as either the cyclic isomer **8** or the open isomer **9**. The computed structures of **7** and **9** and of their etherates are shown in Figures 4 and 5. Searches of the potential energy surfaces in regions with the geometries of **8** and **8**·(OMe_2) led to the respective open isomer. A methyl bridge is obviously too weak to make up for the strain it would cause in **8**. This finding suggests that the methyl bridge in **7** also should be rather weak. When presented with the opportunity to replace the

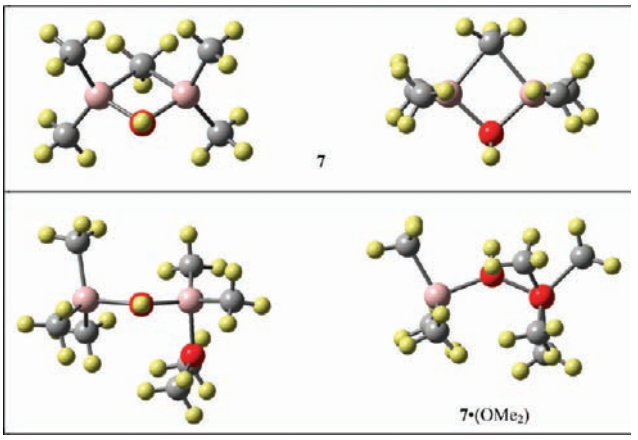

Figure 4. Computed structures of cyclic aggregate **7** formed between DMAH and TMA and its etherate **7**·(OMe_2).

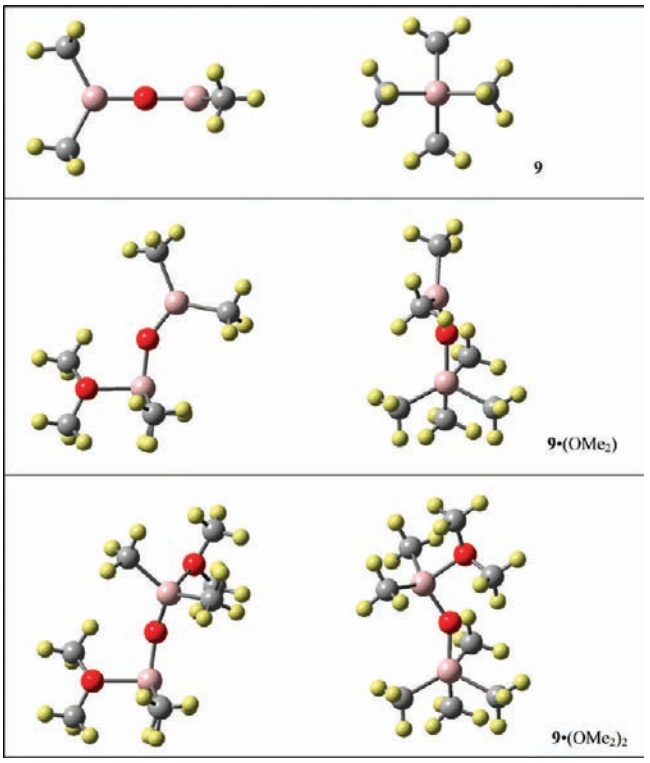

Figure 5. Computed structures of the monomer **9**, its etherate **9**·(OMe_2), and its dietherate **9**·$(OMe_2)_2$.

additional dative bond by the methyl bridge by a Lewis donor molecule, the Me_2Al moiety is expected to opt for the latter, and hence, we considered the structure of the monoetherate **7**·(OMe_2).

As with **4**, cycloadduct **7** has a symmetry plane that includes the OH group; the hydroxyl group is bridging symmetrically with d(O−Al) = 1.884 Å; the hydroxyl-H is out of the plane of the four-membered ring with $\angle$(C···O−H) = 140.6°; and the ring angle at oxygen $\angle$(Al−O(H)−Al) = 93.2° is greater than 90°. The bond lengths of the methyl bridge are d(C−Al) = 2.147 Å, about 10% longer than the exocyclic Al−Me bonds (1.961 Å), and the kite-shaped ring features a ring angle at

Scheme 4. Comparison of the Electronic Structures of Allene, the Typical Heterocumulene CO_2, and the Reversed-Polarity Heterocumulene $O(AlMe_2)_2$, 9

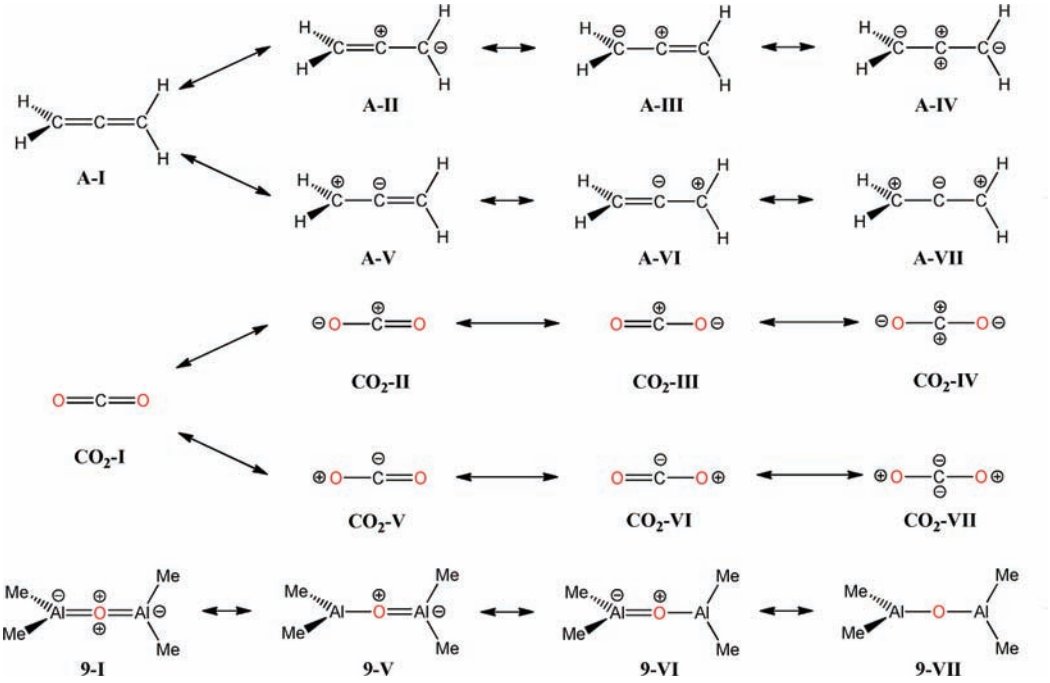

Scheme 5. Bonding in the DMAH Cyclodimer 4, DMAH−TMA Cycloadduct 7, and Some of Their Methane Elimination Products

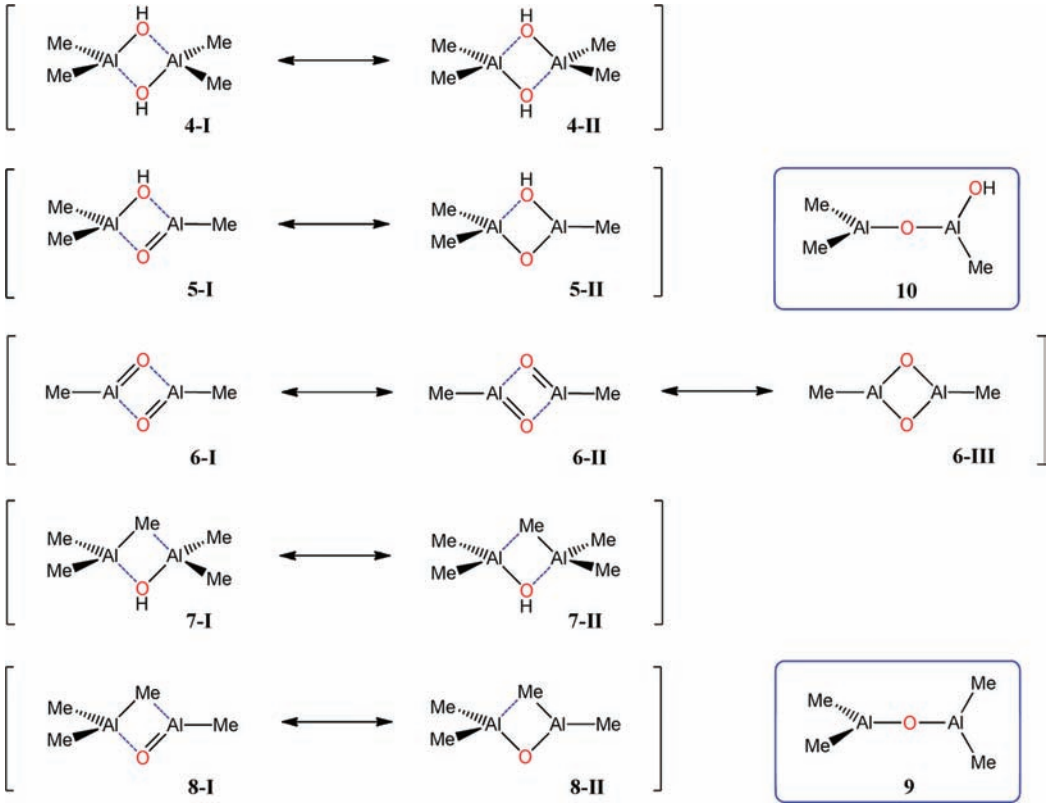

carbon of ∠(Al−Me−Al) = 79.2°. It is not surprising that the methyl bridge of **7** is easily broken by an ether donor to form **7**·(OMe_2), but the thermochemistry of the addition of the Lewis donor to **7** is quite interesting (eq 24). To begin with, the

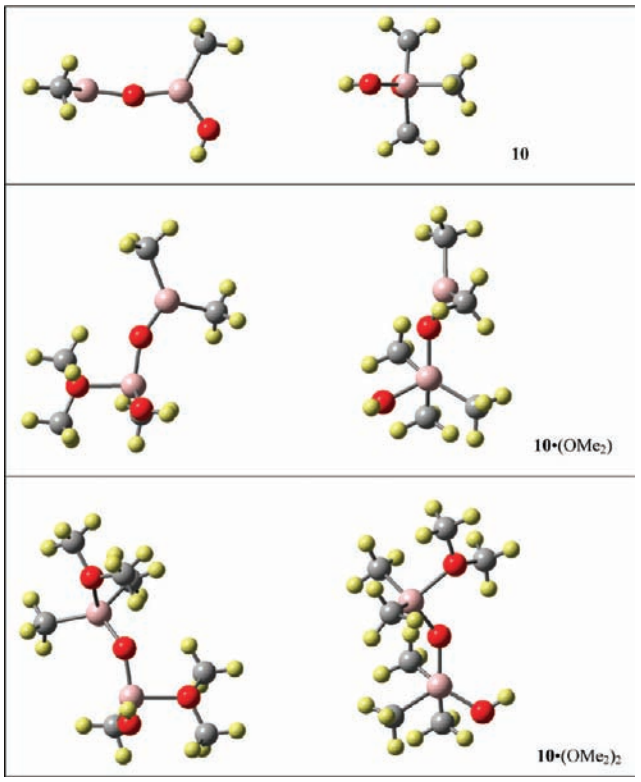

Figure 6. Computed structures of hydroxytrimethyldialuminoxane **10**, its etherate **10**·(OMe_2), and its dietherate **10**·$(OMe_2)_2$.

donor coordination free enthalpy $\Delta G_{298}(7)$ is almost twice as large as $\Delta G_{298}(2)$! Structure **7**·(OMe_2) is TMA-complexed **2**·(OMe_2), and this Lewis acid complexation should *increase* the Lewis acidity of **2**. One would expect stronger complexation of **7** than of **2** for enthalpy reasons. Yet, the ether donor binding energy is much lower for **7** compared to **2** ($\Delta H_{298}(7) > \Delta H_{298}(2)$), and *in spite of this lower enthalpy*, the donor complexation free enthalpy of **7** is much more endergonic than for **2** ($\Delta G_{298}(7) < \Delta G_{298}(2)$). Therefore, the reaction **7** + $OMe_2 \rightarrow$ **7**·(OMe_2) presents a case of entropy-driven binding enhancement caused by the Lewis acid (TMA) complexation. To rationalize this situation, one can argue that the free enthalpy of complexation of **2** by TMA includes a premium because the restriction of internal motions due to the methyl bridging reduces the molecular entropy of the Lewis acid adduct **7**. The ether donor coordination of **7** lifts this restriction, and the dative bond formation thus releases energy previously stored in reduced molecular entropy.

Structure **9** is a reversed-polarity heterocumulene, and this recognition explains the linearity at the central O atom (Scheme 4). The nonpolar canonical structure of the parent allene and its usual heteroanalogues (i.e., CO_2) contains two cumulated double bonds between a divalent four-electron center and two six-electron termini (i.e., A-**I**, CO_2-**I**); the important polar resonance forms **II**−**IV** shift electron density to the termini; and reversed-polarity resonance forms **V**−**VII** play no role. In contrast, cumulene resonance form **I** is highly polar in the case of **9**, and the reversed-polarity resonance forms **V**−**VII** shift electron density to the center and reduce the molecular polarity. The nonpolar structure **9**-**VII** dominates;

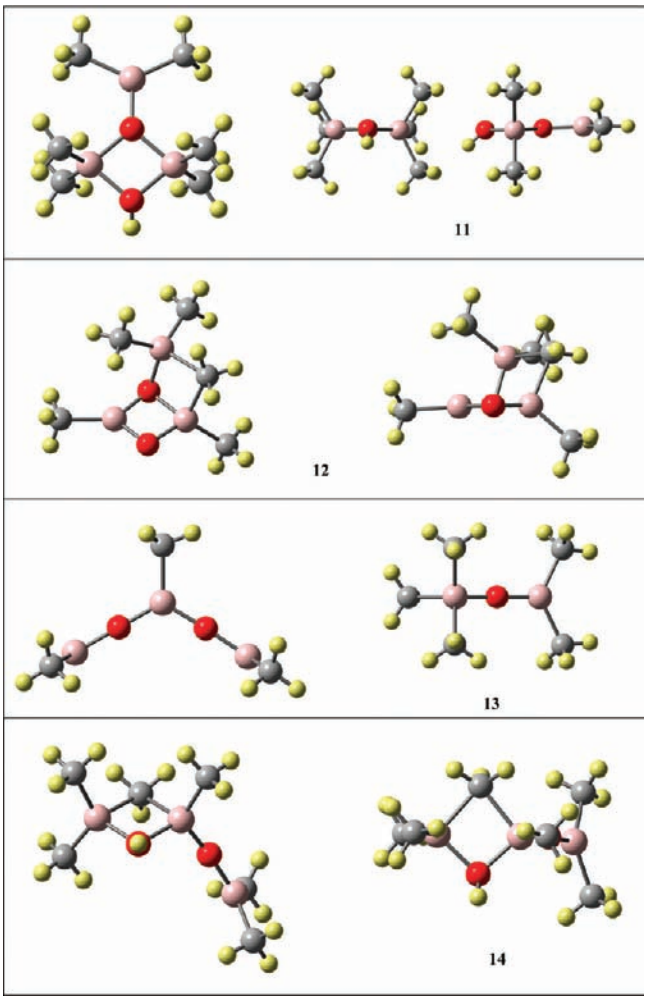

Figure 7. Aggregation of **9** with **2** yields **11**, and CH_4 elimination from **11** affords cyclic and acyclic trialuminoxanes **12** and **13**, respectively. The aggregation of **10** with **1** yields **14**, and CH_4 elimination from **14** also affords the acyclic trialuminoxanes **13**.

the O → Al π-dative bond formations remain partial; and the Al atoms remain the centers of Lewis acidity.

The structure of the pyridine-coordinated *tert*-butyl analogue of **9** has been reported, and its Al_2O moiety is linear in the crystal.[19a] It is an interesting structural feature of **9**·(OMe_2) and **9**·$(OMe_2)_2$ that their bond angles at oxygen remain rather high with 144.7° and 144.3°, respectively. The structures of **9**·$(OMe_2)_n$ also show that ether donor coordination does not cause complete pyramidalization at the Al centers. The strength of the first ether donor coordination in **9** is $\Delta H_{298} = -22.6$ kcal/mol and very close to the ether binding energy $\Delta H_{298} = -22.8$ kcal/mol of **2**, and entropy makes the donor binding of **9** slightly better (eqs 25 and 26).

The methane elimination reaction **7** → **9** + CH_4 (eq 20) is exothermic by $\Delta H_{298} = -8.6$ kcal/mol and exergonic by $\Delta G_{298} = -23.6$ kcal/mol. Primary ether donor complexation favors the elimination product **9**, and we computed $\Delta H_{298} = -37.3$ kcal/mol and $\Delta G_{298} = -37.5$ kcal/mol for reaction **7**·(OMe_2) + $OMe_2 \rightarrow$ **9**·$(OMe_2)_2$ + CH_4 (eq 33).

The free enthalpy of the single CH_4 elimination **7** → **9** + CH_4 (eq 20) is about 26 kcal/mol more exergonic than the single CH_4 elimination **4** → **5** + CH_4 (eq 12), and it is still about 15 kcal/mol

Scheme 6. Heterocumulene 9 Reacts with DMAH to Pentamethyltrialuminoxane 13[a]

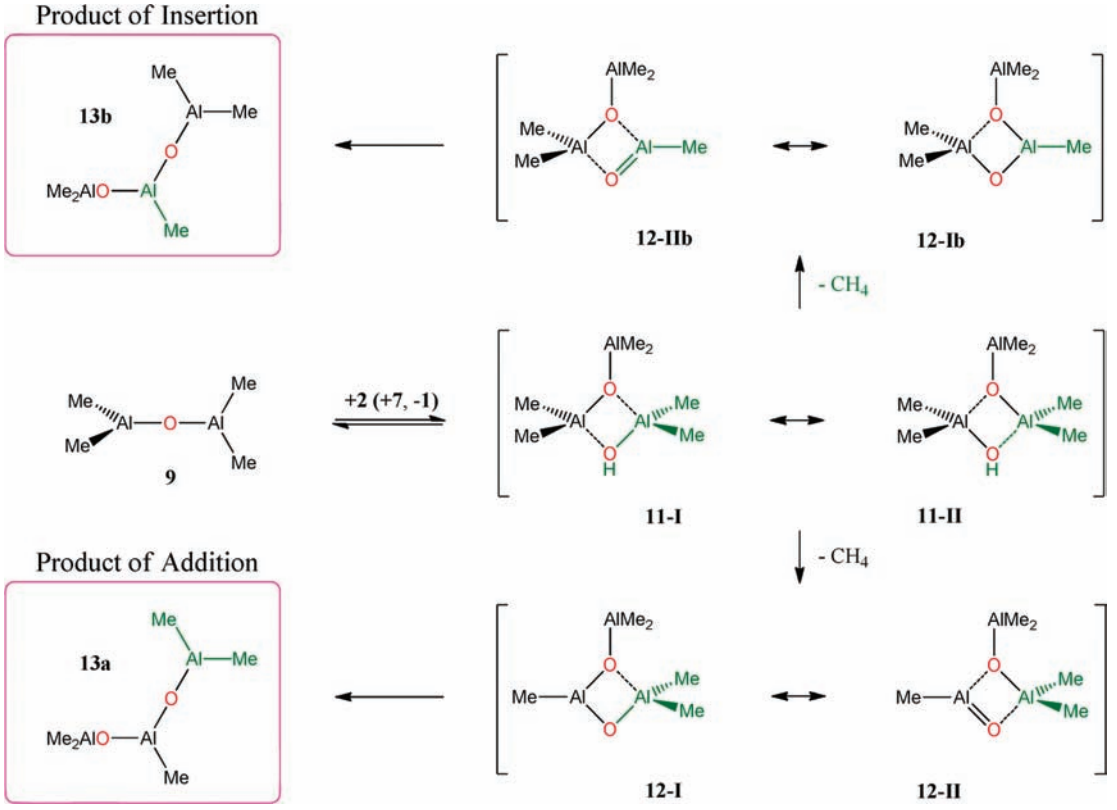

[a] The results are the replacement of a terminal methyl group of **9** by the $OAlMe_2$ moiety of DMAH (shown in green) or the insertion of DMAH's OAlMe moiety into an O—Al bond of **9**.

more exergonic than the double methane elimination **4** → **6** + 2 CH_4 (eq 19). This ordering persists in the presence of a strong Lewis donor, but there are two major differences: First, the free reaction enthalpies of reactions 29 and 33 are almost the same. Second, reaction 27 remains about 22 kcal/mol less exergonic compared to reaction 33, but reaction 27 *definitely becomes exergonic under these conditions*. We thus conclude that product donor stabilization opens the reaction channel leading to **5** and cyclodialuminoxane **6**.

Aggregation Energies and Competition between Cycloadducts 4 and 7. The geometries of **4**—**7** and **9** inform about the bonding of the four-membered rings and their stability toward ring opening and/or fragmentation. The main resonance forms of **4**—**8** are shown in Scheme 5. The bonding in **4** and **7** is best described by hybrids of the degenerate pair of resonance forms **I** and **II**. Structure **5** shows structural features indicative of **5-I** (short bond length of trapez base) and **5-II** (long bond length of trapez base), and the placement of the OH group in the Al_2O_2 plane reflects the dominance of **5-II** (as in derivatives of $MeAl(OH)_2$). Resonance forms **6-I** and **6-II** contribute equally, and **6-III** dominates the bonding of **6**. The bonding of structures in the PES region in the proximity **8** is dominated by **8-II**, and the dative bond is too weak to ensure structural integrity. We know that **5** is a minimum on the potential energy surface and that the dative bond involving the HO donor must be stronger than the dative bond in **7** involving the methyl bridge. Nevertheless, **5-II** indicates that ring opening is an option for **5**, and breaking of the weakest, dative Al···O bond would lead to acyclic **10**. We discuss the significance of this reaction channel below.

There is no question that the products of CH_4 elimination from **4** are much more stable with respect to fragmentation than **4**. The fragmentation reactions **5** → **2** + **3** (eq 35) and **6** → 2 **3** (eq 36) are endergonic by 76.0 and 121.8 kcal/mol, respectively, and the analogous reactions of the ether-coordinated species (eqs 39 and 40) also are endergonic by 63.3 and 103.9 kcal/mol, respectively. Clearly, these fragmentations of **5** and **6** cannot occur under the conditions of typical MAO formation reactions.

There also is no doubt that DMAH would rather dimerize to **4** than form the mixed aggregate **7** with TMA. We find that the dimerization is preferred by about 20 kcal/mol in the absence (eqs 34 and 37) or presence of a Lewis donor (eqs 38 and 42). Moreover, the aggregation energies show that dimer **4** is essentially stable toward fragmentation, whereas the formation of **7** is reversible.

The ratio **4**/**7** therefore should depend on the relative concentrations of **2** and **1**, and the ratio may increase over time. If the hydrolysis of TMA is conducted in such a way as to keep the local concentration of **2** low relative to **1**, then one would expect the formation of aggregate **7** and consequently the production of Sinn monomer **9** by CH_4 elimination. In a TMA hydrolysis process that allowed for a higher relative concentration of **2**, one would expect the formation of dimer **4** and consequently the irreversible production of **5** by methane elimination.

Ring Opening of Cycloadduct 5 to Hydroxytrimethyldialuminoxane 10. We computed the structures of hydroxytrimethyldialuminoxane **10**, of the monoetherate **10**·(OMe_2) formed by unimolecular ring opening of **5**·(OMe_2), and of the

dx.doi.org/10.1021/ja109457j |*J. Am. Chem. Soc.* 2011, 133, 13323–13336

Scheme 7. Hydroxydialuminoxane 10 Employs Its Al−OH Bond to Form Cycloadduct 14 with TMA, and the Reactions via 15 and 16 Present Routes to Pentamethyltrialuminoxane 13

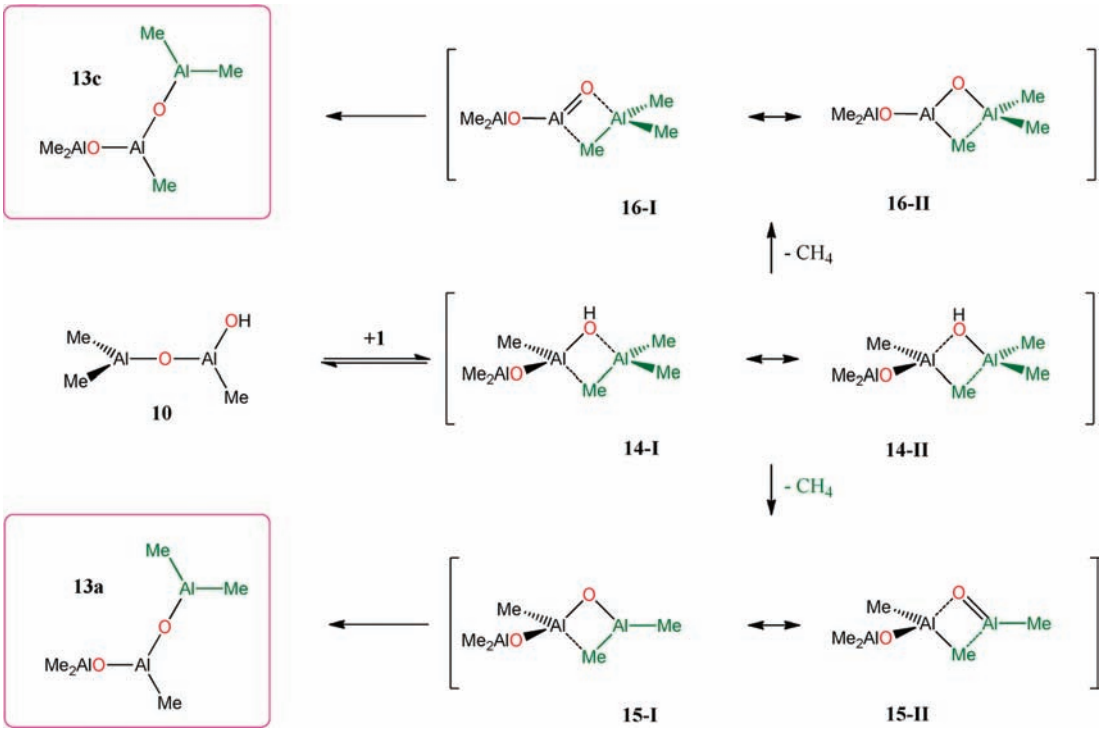

dietherate **10**·$(OMe_2)_2$, and molecular models of these structures are shown in Figure 6.

The ring-opening reaction **5** → **10** is essentially thermoneutral (eq 43), and hence, Lewis donors can affect this reaction in an interesting fashion. The unimolecular ring opening of **5**·(OMe_2) initially leads to **10**·(OMe_2), and subsequent Lewis donor addition then results in **10**·$(OMe_2)_2$. Alternatively, a Lewis donor might assist in the bimolecular ring-opening process Me_2O + **5**·(OMe_2) → **10**·$(OMe_2)_2$. The reaction energy of the unimolecular reaction **5**·(OMe_2) → **10**·(OMe_2) is essentially determined by the difference of the donor binding energies of **5** and **10** (eqs 21 and 44), and this reaction is endergonic (eq 46) by ΔG_{298} = 5.8 kcal/mol. On the other hand, the second donor binding of **10** causes the bimolecular reaction **5**·(OMe_2) + OMe_2 → **10**·$(OMe_2)_2$ to become clearly exergonic with ΔG_{298} = −8.5 kcal/mol (eq 47). Hence, *intermediate* **5** *may have some lifetime if the bimolecular reaction is slowed* by low temperature and/or scarcity of the Lewis donor and the formation of cyclodialuminoxane **6** becomes possible. On the other hand, in an abundance of Lewis donor one must expect the fast, quantitative, and essentially irreversible ring opening of **5** to **10**.

Assessment of Basis Set Effects on Reaction Equilibria. To assess basis set effects on the intrinsic reaction energies, compounds **1**−**10** were computed again at the MP2(full)/6-311G** level. The hydrolysis reaction 1 and the methane elimination reactions 2, 3, and 17−20 are predicted to be significantly harder (less exothermic, more endothermic) at the better theoretical level, whereas the reaction energies for association reactions 34−37 and the ring-opening reaction 43 are less sensitive to theoretical level effects. These effects echo in the reaction energies that include donor complexation and provide additional support for the four key findings:

(1) The reaction free enthalpies for the formations of aggregates **4** and **7** (eqs 38 and 42) are quite similar at levels M1 and M2, and aggregate **4** (ΔG_{298}(38) = −29.2 kcal/mol) is about three times more stable than aggregate **7** (ΔG_{298}(42) = −9.9 kcal/mol).

(2) The reaction free enthalpies for the formations of **5** and **6** (eqs 27 and 29) are markedly less exergonic at the M2 level (ΔG_{298}(27) = −9.0 and ΔG_{298}(29) = −18.8 kcal/mol), whereas the respective value for the formation of **9** is affected much less (ΔG_{298}(30) = −33.1 kcal/mol). The result that matters for the chemistry is the finding that both reactions 27 and 29 are predicted to be quite clearly exergonic at the better level.

(3) The unimolecular and the donor-assisted bimolecular ring-opening reactions of **5** to **10** (eqs 46 and 47) remain endergonic and exergonic, respectively, and the reaction free enthalpies are ΔG_{298}(46) = 3.2 kcal/mol and ΔG_{298}(47) = −11.1 kcal/mol at the better level.

(4) The thermodynamic preference for the formation of **6** over ring opening to **10** (eq 49) is significantly reduced; however, the preference persists, and reaction 49 remains strongly exergonic (ΔG_{298}(49) = −7.2 kcal/mol).

From Dialuminoxane to Tri- and Tetraaluminoxane. We have argued that tetramethyldialuminoxane **9** and hydroxytrimethyldialuminoxane **10** are the main products of CH_4 elimination from aggregate **7** and dimer **4**, respectively, and that the ratio [**4**]/[**7**] depends on the relative concentrations of **2** and **1**. We now consider how the results of our study inform mechanistic discussions of aluminoxane oligomerization.

dx.doi.org/10.1021/ja109457j |*J. Am. Chem. Soc.* 2011, 133, 13323–13336

The reaction of water with an aluminum species involves precoordination of water to the aluminum species and subsequent CH_4 elimination. Since self-aggregating of TMA is at best weak, it is most probable that water reacts with a free TMA molecule rather than with a TMA molecule of **7**. Nonaggregated DMAH is extremely scarce, and hence, a second hydrolysis of DMAH is much less probable than hydrolysis of TMA. The computed aggregation energies further suggest a low probability for direct hydroxylation **9** + H_2O → **10** + CH_4 because any structure with an Al−O bond is capable of forming stable aggregates.

We briefly return to Scheme 5 to clarify the options for CH_4 elimination from the cycloadducts. Aside from single covalent bonds, there are two dative bonds in both resonance forms **I** and **II** of both **4** and **7**; there are two dative bonds and one double bond in resonance forms **I** of **5** and **8**; while form **II** contains only one dative bond; and the resonance forms of **6** feature either two dative bonds and two double bonds or only single bonds. Structures of types **4**, **5**, and **6** can thus be distinguished by the *minimal number of dative bonds* (MNDB) that occur in their resonance forms, and the values are MNDB(**4**) = 2, MNDB(**5**) = 1, and MNDB(**6**) = 0. For an MNDB = 1 structure, the resonance form with just one dative bond indicates the opportune location for facile ring opening. A resonance form with two dative bonds reflects on possible formations and/or fragmentations of the cycloadduct, and fragmentations are likely only if MNDB = 2. In a chain growth reaction with CH_4 elimination, the substrate will be formed by aggregation of two moieties with two dative bonds; the product of CH_4 elimination will have at least one dative bond (MNDB = 1); and the location of that dative bond will indicate the position of the ring opening to afford the chain-elongated acyclic product.

Formally, one can consider any specific CH_4 elimination to occur "across a covalent bond" (i.e., **4-I** → **5-I**, **5-I** → **6-I**, **7-I** → **8-I**) or "across a dative bond" (**4-II** → **5-II**, **5-II** → **6-III**, **7-II** → **8-II**), and the result always is a reduction of MNDB by 1. The latter perspective is convenient because formal elimination across dative bonds directly leads to the MNDB = 1 resonance form of the product. The latter perspective also is physically more appropriate since the structural features suggest that resonance forms with Al═O bonds are minor contributors. The isodesmic reaction **2** + Me−Al═O → **1** + HO−Al═O is endothermic by more than 10 kcal/mol (Table 1), and hence, the contributions of resonance forms with a RO−Al═O moiety should be markedly reduced compared to the contribution of resonance forms that contain a Me−Al═O moiety.

Suppose the initial phase of TMA hydrolysis has occurred, all water has been captured in DMAH and its aggregates, and **9** has been formed (Scheme 6). The aggregation of **9** with DMAH to form **11** (eq 50) is more exothermic than the aggregation of TMA with DMAH in **7** (eq 37). The equilibrium **9** + **7** ⇄ **11** + **1** (eq 52) is therefore exothermic, and aggregate **11** (Figure 7) becomes accessible at least in low concentration. The CH_4 elimination **11** → **12** + CH_4 (eq 53) is analogous to reaction **4** → **5** + CH_4 (eq 17), and one would expect that donor stabilization of the elimination product **12** would be necessary to render the elimination exothermic as with the reaction **4** + OMe_2 → **5**·(OMe_2) + CH_4 (eq 27). Interestingly, our results show that the CH_4 elimination **11** → **12** + CH_4 (eq 53) is exothermic even without donor-stabilization of the product. As can be seen in Figure 7, structure **12** benefits from intramolecular dative bonding between one methyl group of the in-ring $AlMe_2$ moiety and the exocyclic $AlMe_2$ group. An interaction of this kind prior to the CH_4 elimination is precluded because the approach of the exocyclic $AlMe_2$ group to the methyl of one in-ring $AlMe_2$ moiety is sterically impeded by the other in-ring $AlMe_2$ moiety in **11**. The ring opening of **12** trialuminoxane **13** (eq 54) is formally similar to the ring opening of **5** to **10** (eq 43); the free reaction enthalpies of both reactions are less than 1 kcal/mol; and donor stabilization favors the open structures. As with **9**, **13** is a reversed-polarity heterocumulene with essentially linear Al−O−Al units. The OAl_{cent} bonds (1.710 Å) are slightly shorter than the OAl_{term} bonds (1.717 Å) and the OAl bonds (1.718 Å) in **9**.

If one considers the reaction **9** + **2** → **13** formally as a CH_4 elimination across a dative bond of **11-I**, one obtains **12-I**, the MNDB = 1 resonance form of **12**, and cleavage of the dative bond in **12-I** leads to product **13a** with the DMAH's $OAlMe_2$ moiety (shown in green) added to the end of the chain. If one considers the CH_4 elimination across the dative bond of **11-II**, then one obtains **12-Ib**, and ring opening leads to **13b**: the product of insertion of the DMAH's OAlMe moiety into an Al−O bond of **9**. The two endocyclic $AlMe_2$ groups in **11** are chemically equivalent, and there is no reason to assume that the exocyclic $AlMe_2$ moiety would be able to prefer one over the other; hence, the chain elongation proceeds essentially in equal parts by addition (**13a**) and by insertion (**13b**).

Now, suppose that some **10** has been formed in the initial phase of TMA hydrolysis. With the availability of **10**, a variety of reaction channels become viable because **10** may aggregate with any one of its three Al−O bonds, and there may be regiochemical options for CH_4 elimination from the resulting aggregates. Hydroxyaluminoxane **10** can form a **7**-analogue aggregate **14** with TMA, and CH_4 elimination can lead to the formation of trialuminoxane **13** (Scheme 7).

The optimized structure of adduct **14** is shown in Figure 7. One is fully justified to consider **14** as an alternative adduct of **DMAH** of **9**; while the Al−OH bond of **2** coordinates to one of the Al−O bonds of **9** to form **11**, the Al−OH bond of **2** would coordinate an Al−Me bond to form isomer **14**. However, the thermochemical data of eqs 57−59 show that **14** is not accessible by addition of **DMAH** to **9**. The formation of **14** by aggregation of **10** and **TMA** is possible thermodynamically (eqs 60 and 61), and moreover, the equilibrium **10** + **1** ⇄ **14** is driven to the right by the high **TMA** concentrations and by the removal of **14** by the highly exothermic methane elimination and trialuminoxane formation (eq 62). All attempts to find minima of types **15** and **16** on the potential energy surface inadvertently lead to **13**. Structures **8** and **15** are topologically similar, and one would expect the additional O-substituent to further reduce the aluminum's Lewis acidity.

This type of reaction (i.e., **2** → **9**, **10** → **13**) should dominate for any compound with an Al−OH bond in an abundance of TMA. Elimination of methane across the dative bond in **14-I** eliminates one of TMA's methyl groups and leads via **15**-type structures to **13a**, whereas elimination of CH_4 across the dative bond in **14-II** eliminates one of the methyl groups of **9** and leads via **16**-type structures to **13c**, formally the product of TMA addition to Me_2Al−O−Al═O. Cycloadduct **14** is asymmetric; one expects a regiochemical preference; and formation of **13a** should be preferred because contributions by **15-II** (Me−Al═O) are more important than contributions by **16-I** (RO−Al═O).

The minimal mechanism for the growth of oligoaluminoxanes thus involves the homologation of HO-free aluminoxane with

DMAH (i.e., **9** to **13**). Any initially formed hydroxydialuminoxane **10** is easily capped to **13**. The reaction energies of the homologations **9** + **2** → **13** + CH_4 (eq 55) and **2** + **2** → **10** + CH_4 (eq 56) are strikingly similar ($\Delta G_{298} = -42.3 \pm 1.4$ kcal/mol), and the reaction energies of the capping reactions **10** + **1** → **13** + CH_4 (eq 63) and **2** + **1** → **9** + CH_4 (eq 64) also are strikingly similar ($\Delta G_{298} = -45.3 \pm 1.4$ kcal/mol). If trialuminoxane **13** takes the place of **9** in the reaction sequence of Scheme 6, then tetraaluminoxane can be formed in analogy. Hence, our studies are fully consistent with and provide support for Sinn's proposal for the formation of oligoaluminoxanes.

CONCLUSION

If the hydrolysis of TMA is conducted in such a way as to keep the local concentration of **2** low relative to **1** (slow addition of water to TMA solution, vigorous stirring, low temperature, etc.), then one would expect the formation of TMA-DMAH aggregate **7** and consequently the production of Sinn monomer **9** by CH_4 elimination. Homologation via **7**-analogue **9**-DMAH aggregates affords trialuminoxanes **13**, and higher aluminoxanes are then accessible in analogy.

In a process for TMA hydrolysis that would allow for a higher relative concentration of **2** (fast addition of water to TMA solution, etc.; slow addition of TMA solution to water, etc.), one would expect the formation of the rather stable DMAH dimer **4** and consequently the production of **5** by CH_4 elimination. The simplest outcome would occur under reaction conditions that favor the ring opening of **5** to **10** and the subsequent capping of **10** with TMA to form **13**. Since the homologation of **9** provides the same outcome, the path via **10** cannot be excluded.

Our structural studies suggest that the formation of cyclodialuminoxane **6** is thermodynamically possible under reaction conditions that (a) provide product stabilization to **6** and that (b) grant **5** some lifetime. There is an apparent dilemma here in that Lewis donors facilitate the ring opening of **5**, but we believe that this challenge can be addressed. In the presence of a sterically demanding donor, for example, it should be possible to slow the bimolecular ring opening of **5** without lowering the product stabilization of **6**. We have employed dimethylether merely as a simple model of a donor molecule, and the important donors in MAO chemistry (halides, sulfates, etc. used in MAO production; oxygen in aluminoxanes, ...) remain to be identified.

Dialuminoxanes **9** and **10** are reversed-polarity heterocumulenes, and O → Al dative bonding reduces the Lewis donor ability of the central oxygen in acyclic aluminoxanes toward Lewis acids. The bond angle at oxygen remains above 140° in **9**·$(OMe_2)_2$ and **10**·$(OMe_2)_2$; that is, intramolecular dative binding in **9** and **10** competes successfully with Al-complexation by the ether donors! In cyclodialuminoxane **6**, on the other hand, intramolecular O → Al dative bonding is impeded, and the dicoordinate oxygen in **6** is a strong Lewis donor. The Lewis donor strength at oxygen is significantly different for acyclic and cyclic dialuminoxanes, and this difference in their electronic structures has important consequences for the chemistry in the presence of Lewis acids with high oxophilicity. Oxophilic Lewis acids may provide additional product stabilization to cycloaluminoxanes in the course of MAO formation. Alkali metal ions are known for their high oxophilicity,[42] and alkali metal salts are added in some processes for MAO formation.[16] More importantly, the ethylene polymerization catalysts all contain highly oxophilic transition metals,[43] and our studies suggest that these transition metal catalysts should discriminate strongly in favor of cycloaluminoxane-O donors even if these are present only in small concentrations in the MAO cocatalyst.

ASSOCIATED CONTENT

Supporting Information. Tables of total energies and thermochemical data computed at MP2(full)/6-31G* and MP2-(full)/6-311G** and Cartesian coordinates of stationary structures. This material is available free of charge via the Internet at http://pubs.acs.org.

AUTHOR INFORMATION

Corresponding Author
glaserr@missouri.edu

ACKNOWLEDGMENT

MU Research Computing is supported by NASA Funding and additional support from Dell, SGI, Sun Microsystems, TimeLogic, and Intel.

REFERENCES

(1) (a) Ziegler, K. *Angew. Chem.* **1964**, *76*, 545–553. (b) Natta, G. *Angew. Chem.* **1964**, *76*, 553–566.

(2) (a) Nowlin, T. E.; Mink, R. I.; Kissin, Y. V. *Handb. Trans. Met. Polym. Catal.* **2010**, 131–155. (b) Severn, J.; Jones, R. L. *Handb. Trans. Met. Polym. Catal.* **2010**, 157–230.

(3) (a) Guertzgen, S.; Schneider, J.; Schrader, R. *Eur. Pat. Appl.* 1993, 6 p.; EP 93-103725. (b) Eisenberg, D. C.; Pradhan, M. M.; Howie, M. S. *Process for preparing trimethylaluminum*. U.S. Pat. Appl. 1996, 5 p.; US 95-436695.

(4) (a) Sinn, H.; Kaminsky, W. *Adv. Organomet. Chem.* **1980**, *18*, 99–149. (b) Andresen, A.; Cordes, H. G.; Herwig, J.; Kaminsky, W.; Merck, A.; Mottweiler, R.; Pein, J.; Sinn, H.; Vollmer, H. J. *Angew. Chem.* **1976**, *88*, 689–690.

(5) Severn, J. *Tailor-Made Polym.* **2008**, 95–138.

(6) Köppl, A.; Alt, H. H.; Phillips, M. D. *J. Appl. Polym. Sci.* **2001**, *80*, 454–466.

(7) (a) Small, B. L.; Brookhart, M.; Bennett, A. M. A. *J. Am. Chem. Soc.* **1998**, *120*, 4049–4050. (b) Small, B. L.; Brookhart, M. *J. Am. Chem. Soc.* **1998**, *120*, 7143–7144.

(8) Ittel, S. D.; Johnson, L. K.; Brookhart, M. *Chem. Rev.* **2000**, *100*, 1169–1203.

(9) Britovsek, G. J. P.; Gibson, V. C.; Kimberley, B. S.; Maddox, P. J.; McTavish, S. J.; Solan, G. A.; White, A. J. P.; Williams, D. J. *Chem. Commun.* **1998**, 849–850.

(10) Zhang, T.; Sun, W. H.; Li, T.; Yang, X. *J. Mol. Catal. A* **2004**, *218*, 119–124.

(11) Zhang, S.; Sun, W.-H.; Xiao, T.; Hao, X. *Organometallics* **2010**, *29*, 1168–1173.

(12) Guo, D.; Han, L.; Zhang, T.; Sun, W. H.; Li, T.; Yang, X. *Macromol. Theory Simul.* **2002**, *11*, 1006–1012.

(13) Zhang, T.; Guo, D.; Jie, S.; Sun, W.-H.; Li, T.; Yang, X. *J. Polym. Sci., Part A* **2004**, *42*, 4765–4774.

(14) Zuo, W.; Sun, W.-H.; Zhang, S.; Hao, P.; Shiga, A. *J. Polym. Sci., Part A* **2007**, *45*, 3415–3430.

(15) Suzuki, Y.; Kinoshita, S.; Shibahara, A.; Ishii, S.; Kawamura, K.; Inoue, Y.; Fujita, T. *Organometallics* **2010**, *29*, 2394–2396.

(16) (a) Sinn, H.; Kaminsky, W.; Vollmer, H. J.; Woldt, R. *Polyethylene, polypropylene, and ethylene-propylene copolymers*. European Patent DE3007725 (A1), 1981. (b) Sinn, H.; Kaminsky, W.; Vollmer, H. J.; Woldt, R. *Preparing Ethylene Polymers Using Ziegler Catalysts*

Comprising Cyclodienyl Compound of Zirkonium. U.S. Patent 4,404,344, Sept. 1983.

(17) (a) Sangokoya, S. A. *Preparation of aluminoxanes*. U.S. Patent 5099050, March 1992. (b) Sangokoya, S. A.; Howie, M. S.; Dunaway, A. L. *Hydrocarbon solutions of alkylaluminoxane compounds*. U.S. Patent 5157008, Oct. 1992.

(18) Barron, A. R. *Macromol. Symp.* **1995**, *97*, 15–25.

(19) (a) Mason, M. R.; Smith, J. M.; Bott, S. G.; Barron, A. R. *J. Am. Chem. Soc.* **1993**, *115*, 4971–4984. (b) Harlan, C. J.; Mason, M. R.; Barron, A. R. *Organometallics* **1994**, *13*, 2957–2969.

(20) Watanabi, M.; McMahon, C. N.; Harlan, C. J.; Barron, A. R. *Organometallics* **2001**, *20*, 460–467.

(21) Pasynkiewicz, S. *Polyhedron* **1990**, *9*, 429–453.

(22) Sinn, H. J. *Macromol. Symp.* **1995**, *97*, 27–52.

(23) Zurek, E.; Woo, T. K.; Firman, T. K.; Ziegler, T. *Inorg. Chem.* **2001**, *40*, 361–370.

(24) Negureanu, L.; Hall, R. W.; Butler, L. G.; Simeral, L. A. *J. Am. Chem. Soc.* **2006**, *128*, 16816–16826.

(25) (a) Linnolahti, M.; Severn, J. R.; Pakkanen, T. A. *Angew. Chem., Int. Ed.* **2008**, *47*, 9279–9283. (b) Linnolahti, M.; Severn, J. R.; Pakkanen, T. A. *Angew. Chem., Int. Ed.* **2006**, *45*, 3331–3334.

(26) E. Maréchal, E.; Wilks, E. S. *Pure Appl. Chem.* 2001, *73*, 1511. http://www.iupac. org/publications/pac/73/9/1511/ (accessed July 7, 2010).

(27) *Nomenclature of Inorganic Chemistry: IUPAC Recommendations*; Connelly, N. G., Damhus, T., Eds.; Royal Society of Chemistry, 2005. http://old.iupac.org/publications/ books/rbook/Red_Book_2005.pdf (accessed July 7, 2010). (a) IR-6.2.4.2 Hydrides consisting of chains of alternating skeletal atoms. (b) IR-6.3.1 Use of suffixes and prefixes. (c) IR-6.2.4.3 Heteronuclear monocyclic parent hydrides.

(28) Phan, T. B.; Breugst, M.; Mayr, H. *Angew. Chem., Int. Ed.* **2006**, *45*, 3869–3874.

(29) Linton, D. J.; Wheatley, A. E. H. *Struct. Bonding (Berlin)* **2003**, *105*, 67–139.

(30) (a) Gritzner, G. *J. Mol. Liq.* **1997**, *73*−*74*, 487–500. (b) Sandstroem, M.; Persson, I.; Persson, P. *Acta Chem. Scand.* **1990**, *44*, 653–675.

(31) Frisch, M. J. et al. *Gaussian 03*, Revision E.01; Gaussian, Inc.: Wallingford CT, 2004.

(32) Peng, C.; Ayala, P. Y.; Schlegel, H. B.; Frisch, M. J. *J. Comput. Chem.* **1996**, *17*, 49–56.

(33) (a) Wilson, S. *Handb. Mol. Phys. Quantum Chem.* **2003**, *2*, 314–373. (b) Pople, J. A. *Rev. Modern Phys.* **1999**, *71*, 1267–1274.

(34) (a) Cook, D. B. *Handbook of Computational Quantum Chemistry*; Dover Publications: Mineola, NY, 2005. (b) Schatz, G. C.; Ratner, M. A. *Quantum Mechanics in Chemistry*; Dover Publications: Mineola, NY, 2002.

(35) For this comparison, the back reaction 43 was considered, i.e., the formation of **5** from **10**.

(36) Henrickson, C. H.; Duffy, D.; Eyman, D. P. *Inorg. Chem.* **1968**, *7*, 1047–1051.

(37) Haaland, A.; Samdal, S.; Stokkeland, O.; Weidlein, J. *J. Organomet. Chem.* **1977**, *134*, 165–171.

(38) McMahon, C. N.; Bott, S. G.; Barron, A. R. *J. Chem. Soc., Dalton Trans.* **1997**, 3129–3137.

(39) Almenningen, A.; Halvorsen, S.; Haaland, A. *Acta Chem. Scand.* **1971**, *25*, 1937–1945.

(40) Balasubramanian, S.; Mundy, C. J.; Klein, M. L. *J. Phys. Chem. B* **1998**, *102*, 10136–10141.

(41) Rogers, J. H.; Apblett, A. W.; Cleaver, W. M.; Tyler, A. N.; Barron, A. B. *J. Chem. Soc., Dalton Trans.* **1992**, 3179–3187.

(42) Wheatley, A. E. H. *Chem. Soc. Rev.* **2001**, *30*, 265–273.

(43) Carpentier, J.-F. *Dalton Trans.* **2010**, *39*, 37–48.